Supplement of Clim. Past, 16, 2183–2201, 2020
https://doi.org/10.5194/cp-16-2183-2020-supplement
© Author(s) 2020. This work is distributed under
the Creative Commons Attribution 4.0 License.

Climate of the Past
Open Access

Supplement of

Simulating Marine Isotope Stage 7 with a coupled climate–ice sheet model

Dipayan Choudhury et al.

Correspondence to: Dipayan Choudhury (dipayanc@pusan.ac.kr)

The copyright of individual parts of the supplement might differ from the CC BY 4.0 License.

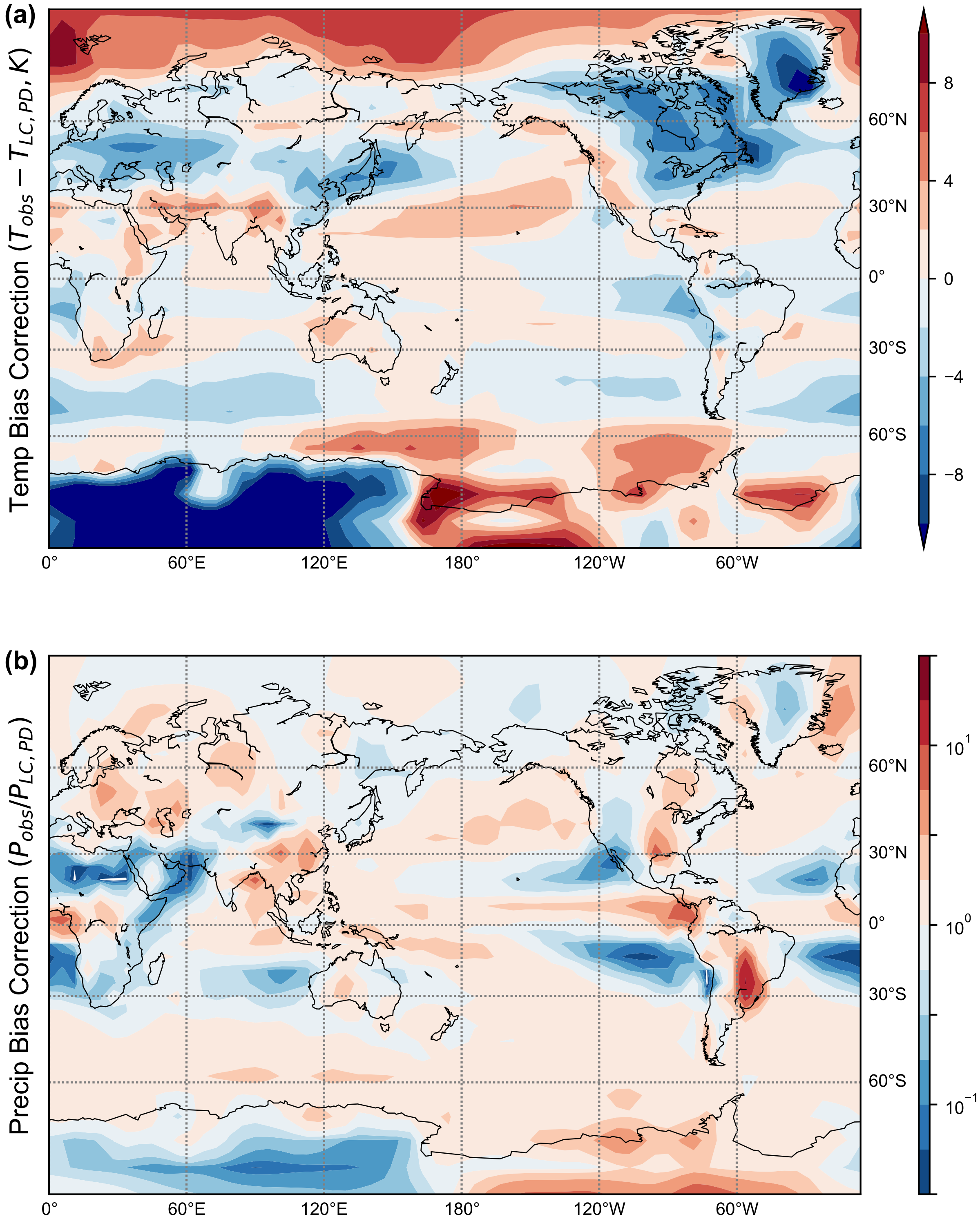

Figure S1: Bias correction used for LOVECLIM outputs. (a) Additive bias correction for annual mean surface temperature (K). (b) Multiplicative bias correction for annual mean precipitation. Colours are log normalised for the precipitation case.

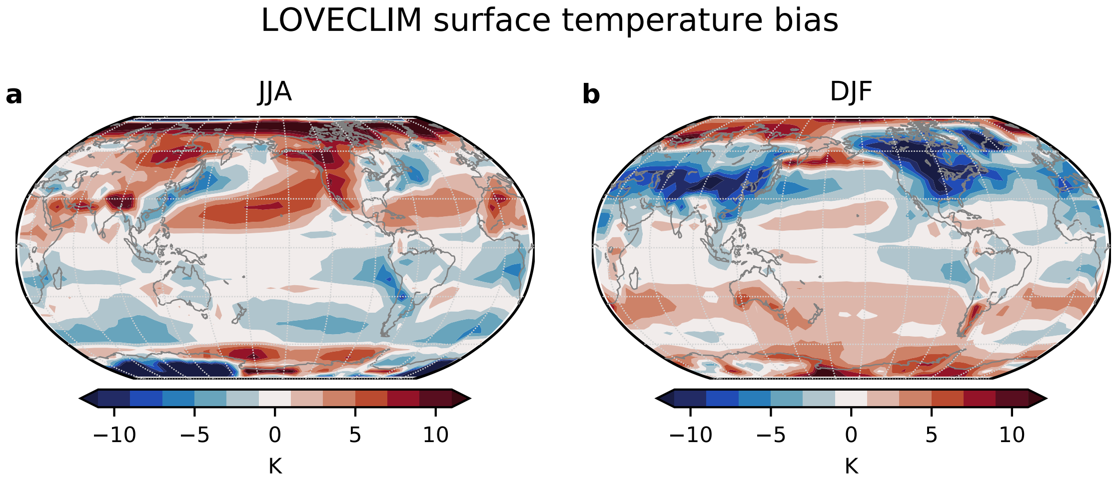

Figure S2: Seasonal biases in surface temperature (K) from LOVECLIM for (a) JJA, and (b) DJF.

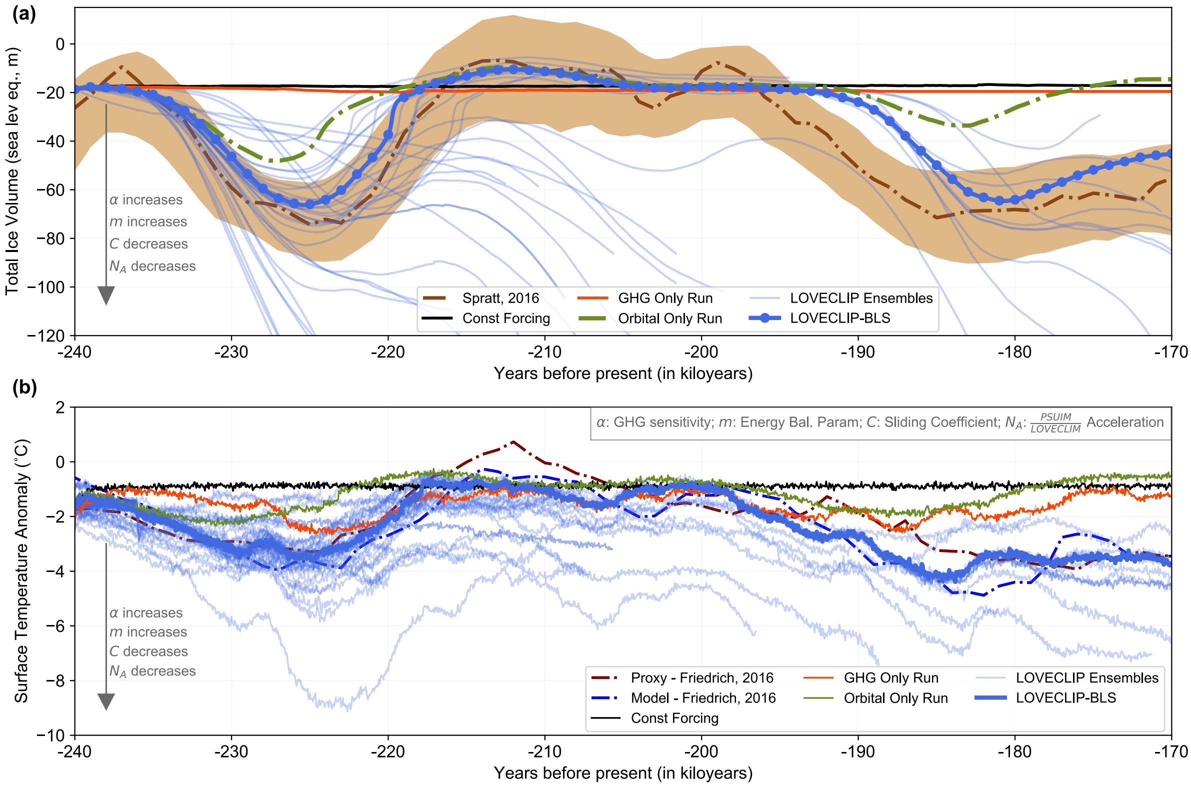

Figure S3: Transient LOVECLIP ensemble simulations over MIS7 with varying GHG sensitivities (α = 1.5-3.5), energy balance parameter (m = 80-150Wm-2), basal sliding coefficient (C = 10^{-6}-10^{-8} myr-1Pa-2) and PSUIM-vs-LOVECLIM acceleration factor (N_A = 1,2,5,10,20). The best results are obtained for α=2, m=125 Wm^{-2}, binary sliding map (ocean: C=10^{-6} myr^{-1}Pa^{-2} and land: C=10^{-8} myr^{-1}Pa^{-2}) and N_A=5 (experiment 1 in Table 1, BLS).

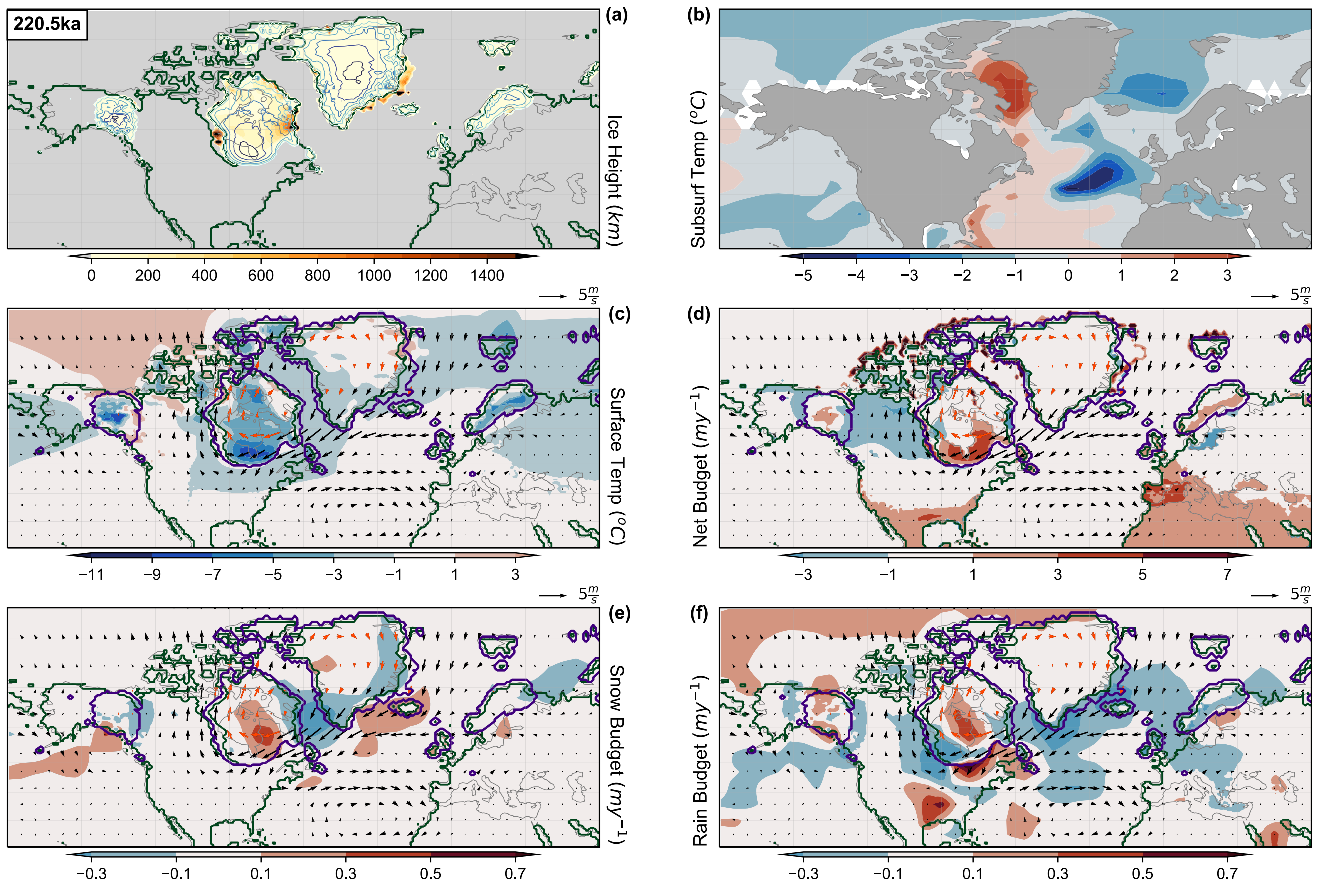

Figure S4: Simulated climate anomalies at 220.5ka over the Laurentide region. Anomalies here are with respect to the initial condition at 240ka. (a) Simulated anomalies in basal ice velocity (solid colors, my^{-1}), ice thickness (colored contours, *km*, contour levels same as in Fig. 4) and the grounding line (solid green lines). (b) Subsurface ocean temperature anomalies (˚C) at 400m depth. (c) Surface temperature anomalies (˚C) overlaid with anomalous wind vectors at 800hPa (ms^{-1}). The winds over regions with ice thickness greater than one km are plotted in red. (d) Net mass balance anomalies (my^{-1}) overlaid with anomalous winds (ms^{-1}). (e) Snowfall anomalies (my^{-1}) overlaid with *absolute* winds (ms^{-1}). (f) Rainfall anomalies (my^{-1}) overlaid with *anomalous* winds (ms^{-1}). The purple line in (c) to (f) mark the boundaries of the ice sheets and ice shelves. Anomalies over the Eurasian ice sheet are small and not shown.

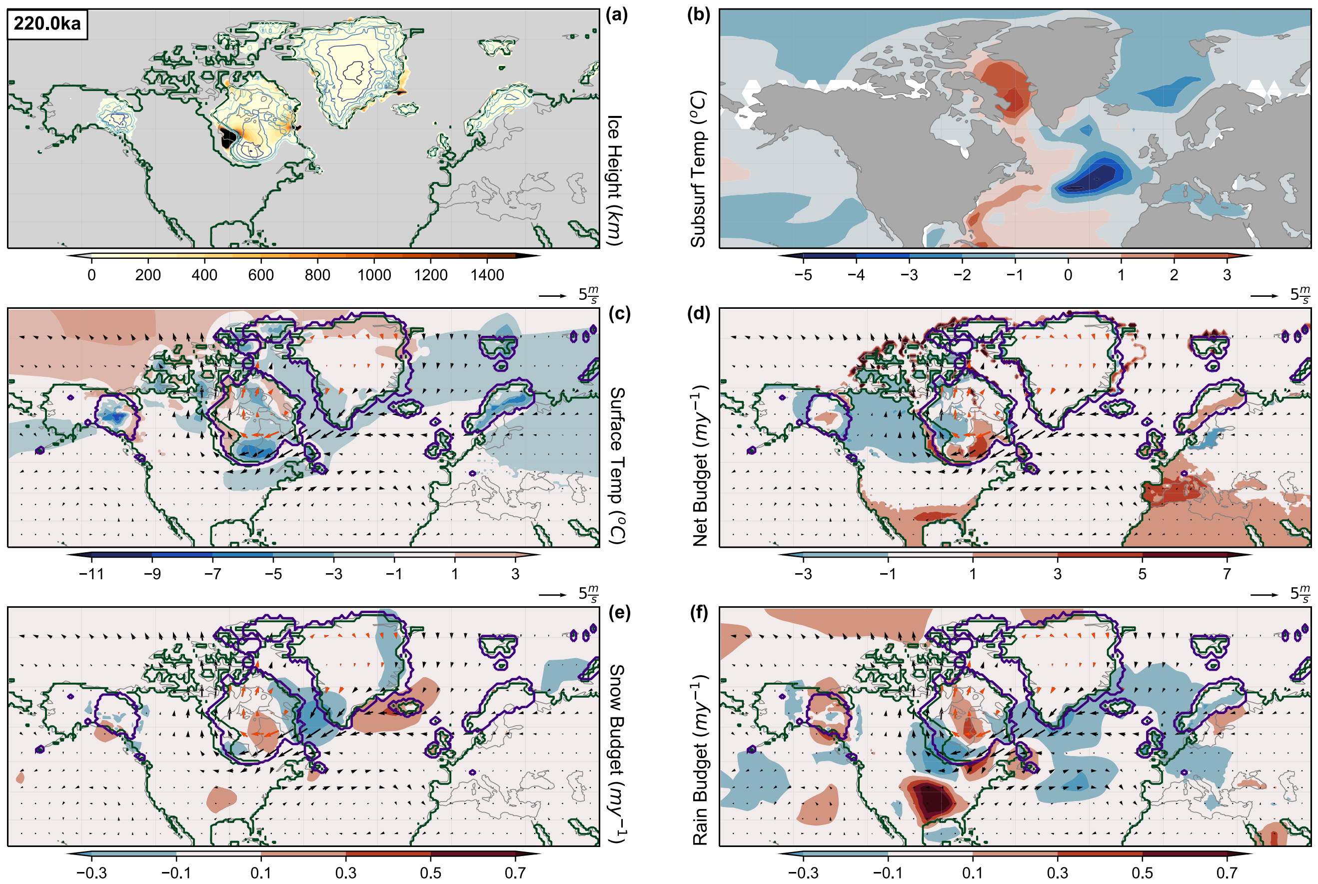

Figure S5: Simulated climate anomalies at 220.0ka over the Laurentide region. Anomalies here are with respect to the initial condition at 240ka. (a) Simulated anomalies in basal ice velocity (solid colors, my^{-1}), ice thickness (colored contours, *km*, contour levels same as in Fig. 4) and the grounding line (solid green lines). (b) Subsurface ocean temperature anomalies (°C) at 400m depth. (c) Surface temperature anomalies (°C) overlaid with anomalous wind vectors at 800hPa (ms^{-1}). The winds over regions with ice thickness greater than one km are plotted in red. (d) Net mass balance anomalies (my^{-1}) overlaid with anomalous winds (ms^{-1}). (e) Snowfall anomalies (my^{-1}) overlaid with *absolute* winds (ms^{-1}). (f) Rainfall anomalies (my^{-1}) overlaid with *anomalous* winds (ms^{-1}). The purple line in (c) to (f) mark the boundaries of the ice sheets and ice shelves. Anomalies over the Eurasian ice sheet are small and not shown.

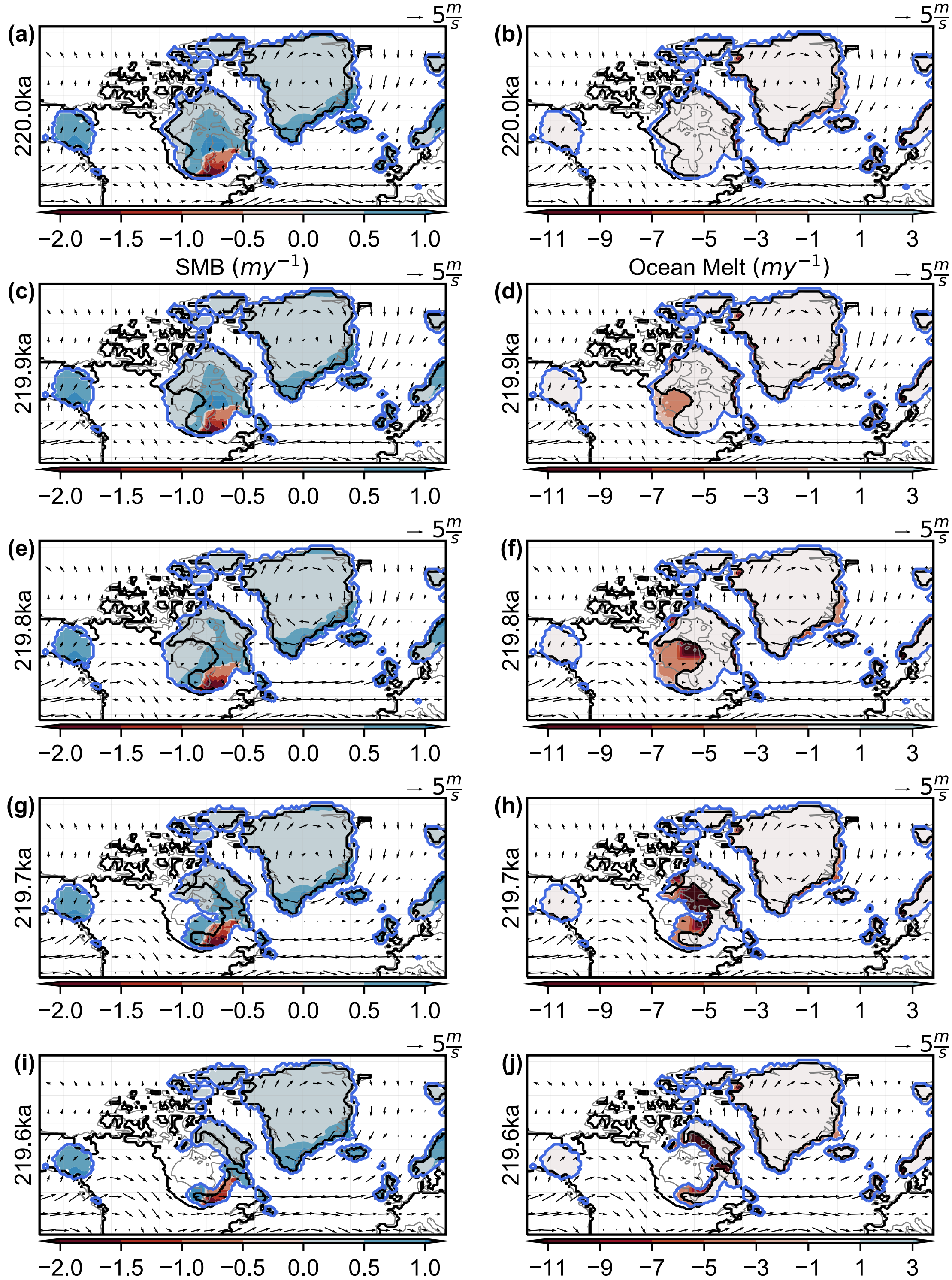

Figure S6: Temporal snapshots around the spikes in SMB and Ocean melt of Figure 6h and 6i (~15ky relative time of the dashed lines, corresponds to ~ 220ka in real time). Simulated surface mass balance (left column) and subshelf melt (right column) values at (a,b) 220ka, (c,d) 219.9ka, (e,f) 219.8ka, (g,h) 219.7ka and (I,j) 219.6ka. The blue lines mark the boundaries of the ice sheets and the black lines show the grounding line.

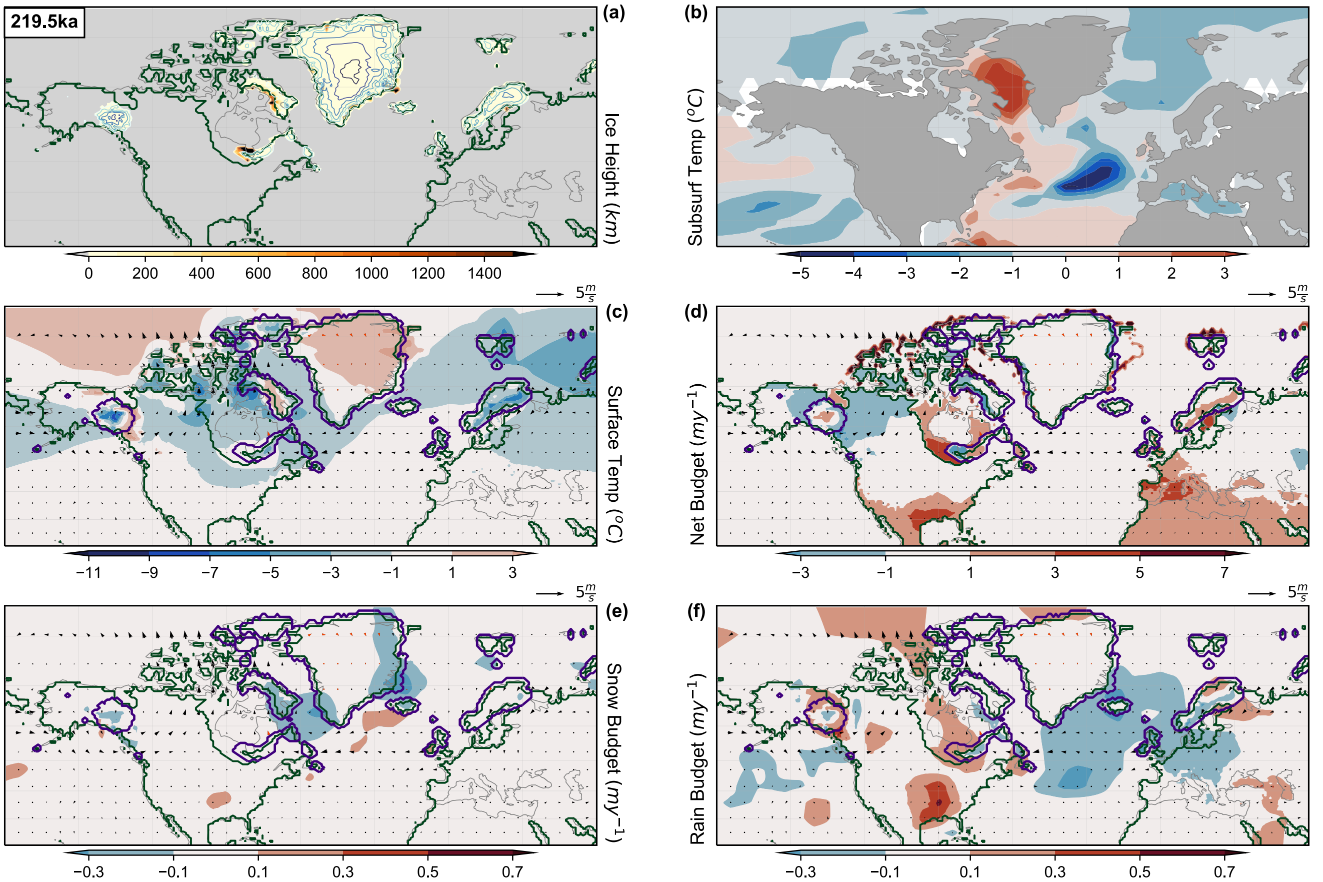

Figure S7: Simulated climate anomalies at 219.5ka over the Laurentide region. Anomalies here are with respect to the initial condition at 240ka. (a) Simulated anomalies in basal ice velocity (solid colors, my^{-1}), ice thickness (colored contours, *km*, contour levels same as in Fig. 4) and the grounding line (solid green lines). (b) Subsurface ocean temperature anomalies (˚C) at 400m depth. (c) Surface temperature anomalies (˚C) overlaid with anomalous wind vectors at 800hPa (ms^{-1}). The winds over regions with ice thickness greater than one km are plotted in red. (d) Net mass balance anomalies (my^{-1}) overlaid with anomalous winds (ms^{-1}). (e) Snowfall anomalies (my^{-1}) overlaid with *absolute* winds (ms^{-1}). (f) Rainfall anomalies (my^{-1}) overlaid with *anomalous* winds (ms^{-1}). The purple line in (c) to (f) mark the boundaries of the ice sheets and ice shelves. Anomalies over the Eurasian ice sheet are small and not shown.

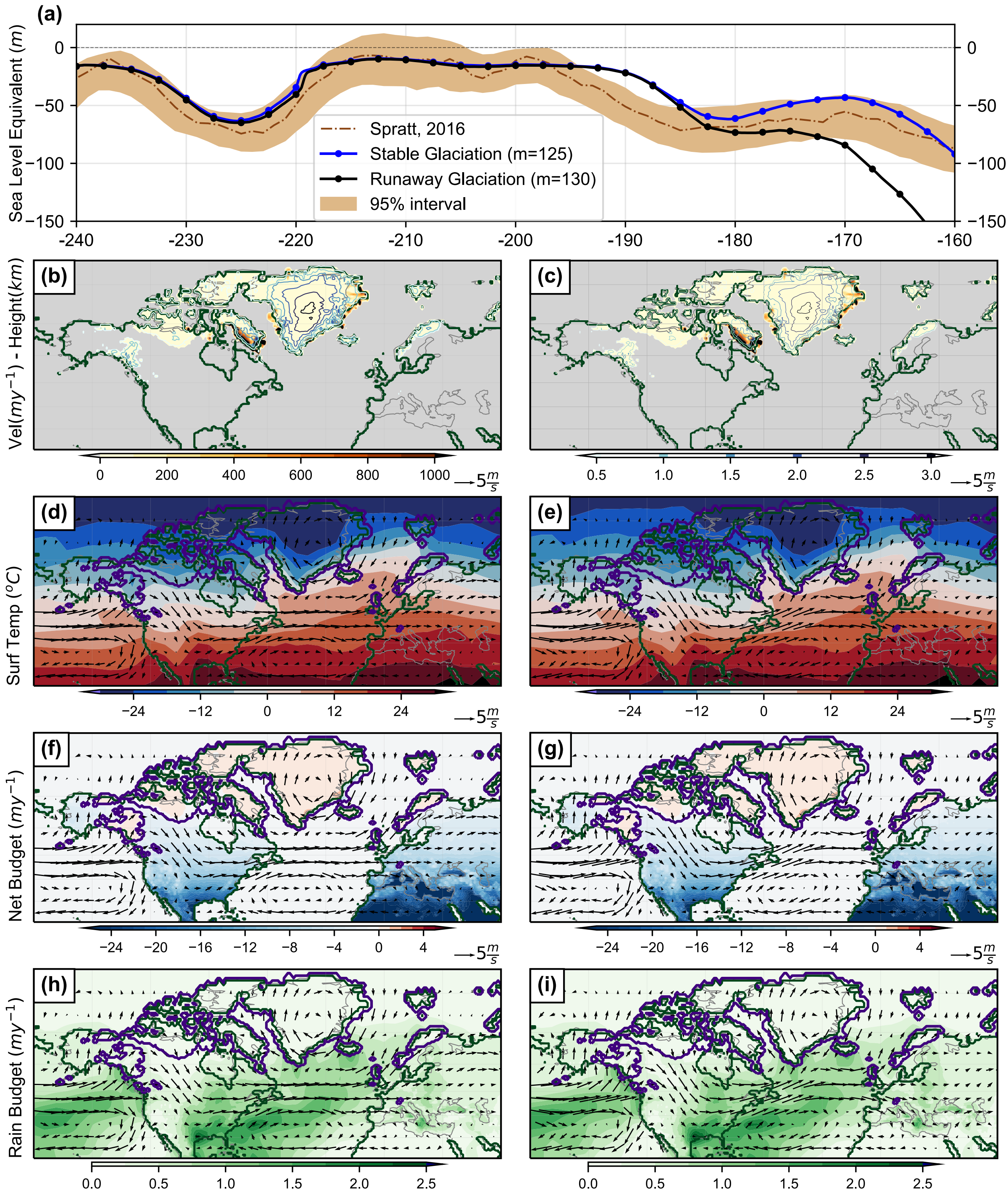

Figure S8: Initial values of climate and ice sheet variables at 240ka. (a) Sea level reconstruction (m) and 95% confidence interval of Spratt and Lisiecki (2016) (brown). Total ice volume (in terms of SLE, m) from two ensemble members of LOVECLIP, one that leads to a stable glacial inception (blue; α=2, m=125 Wm^{-2}) and another into a runaway glaciation (black; α=2, m=130 Wm^{-2}). Climate and ice sheet variables at 240ka from the stable glaciation on the left column (b, d, f and h) and runaway glaciation on the right (c, e, g and i). (b,c) Basal ice velocity (solid colors, my^{-1}) overlaid with ice thickness (colored contours, km) and the grounding line (solid green lines). (d,e) Surface temperature (°C) overlaid with wind vectors at 800hPa (ms^{-1}). (f,g) Net mass balance (my^{-1}) overlaid with winds (ms^{-1}). (h,i) Net accumulation (my^{-1}) overlaid with winds (ms^{-1}). The purple contours in (d) to (i) mark the boundaries of the ice sheets from each run (stable for left and runaway for right).

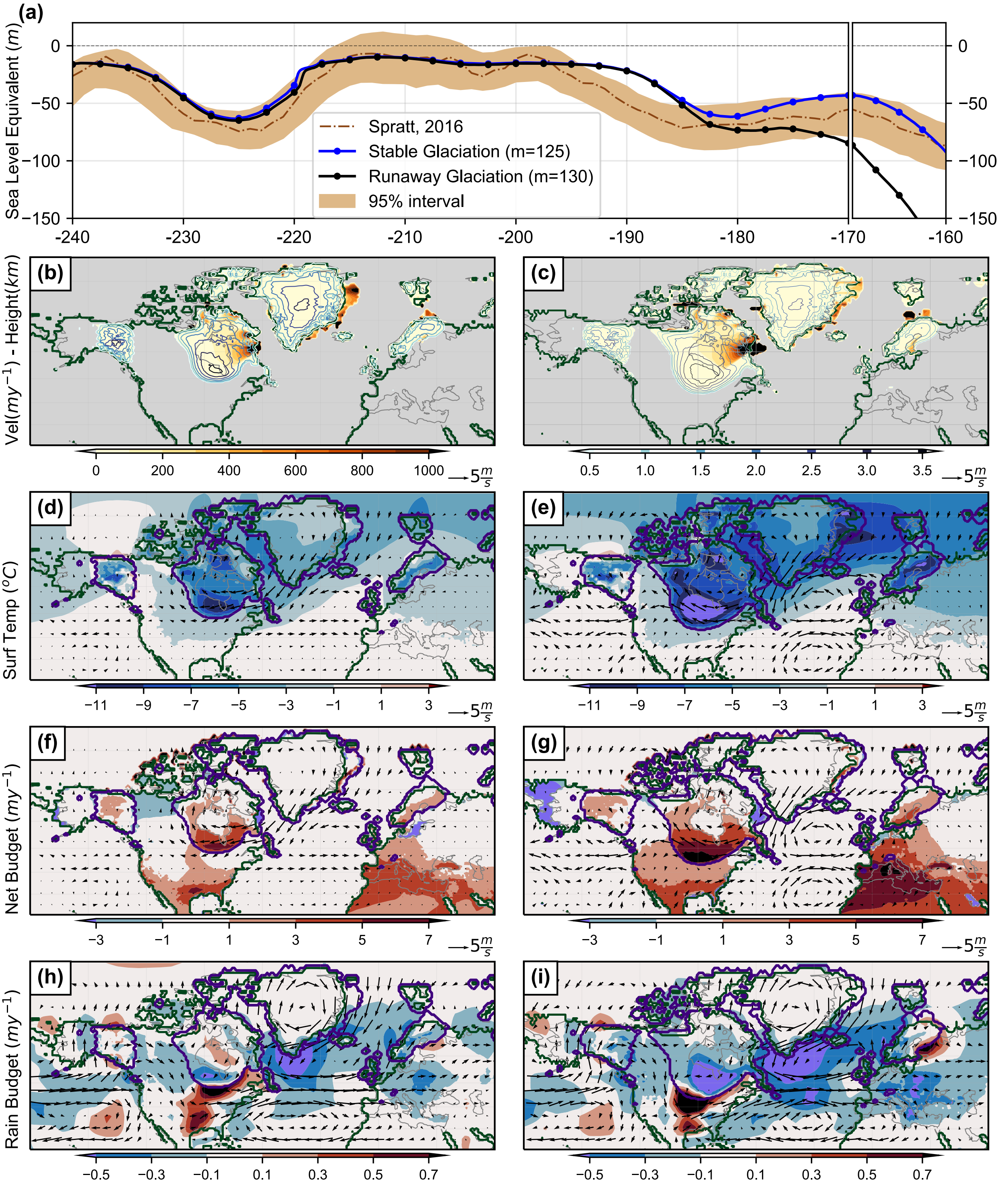

Figure S9: Bifurcation of the system at 170ka while transitioning into MIS 6 over Laurentide. (a) Sea level reconstruction (m) and 95% confidence interval of Spratt and Lisiecki (2016) (brown). Total ice volume (in terms of SLE, m) from two ensemble members of LOVECLIP, one that leads to a stable glacial inception (blue; α=2, m=125 Wm^{-2}) and another into a runaway glaciation (black; α=2, m=130 Wm^{-2}). Climate and ice sheet variables at 170ka from the stable glaciation on the left column (b, d, f and h) and runaway glaciation on the right (c, e, g and i). (b,c) Basal ice velocity (solid colors, my^{-1}) overlaid with ice thickness (colored contours, km) and the grounding line (solid green lines). (d,e) Surface temperature anomalies (*˚C*) overlaid with *anomalous* wind vectors at 800hPa (ms^{-1}). (f,g) Net mass balance anomalies (my^{-1}) overlaid with *anomalous* winds (ms^{-1}). (h,i) Rainfall anomalies (my^{-1}) overlaid with *absolute* winds (ms^{-1}). The purple contours in (d) to (i) mark the boundaries of the ice sheets from each run (stable for left and runaway for right). Anomalies here are with respect to the initial condition at 240ka. Anomalies over the Eurasian and Siberian ice sheets are small and not shown.

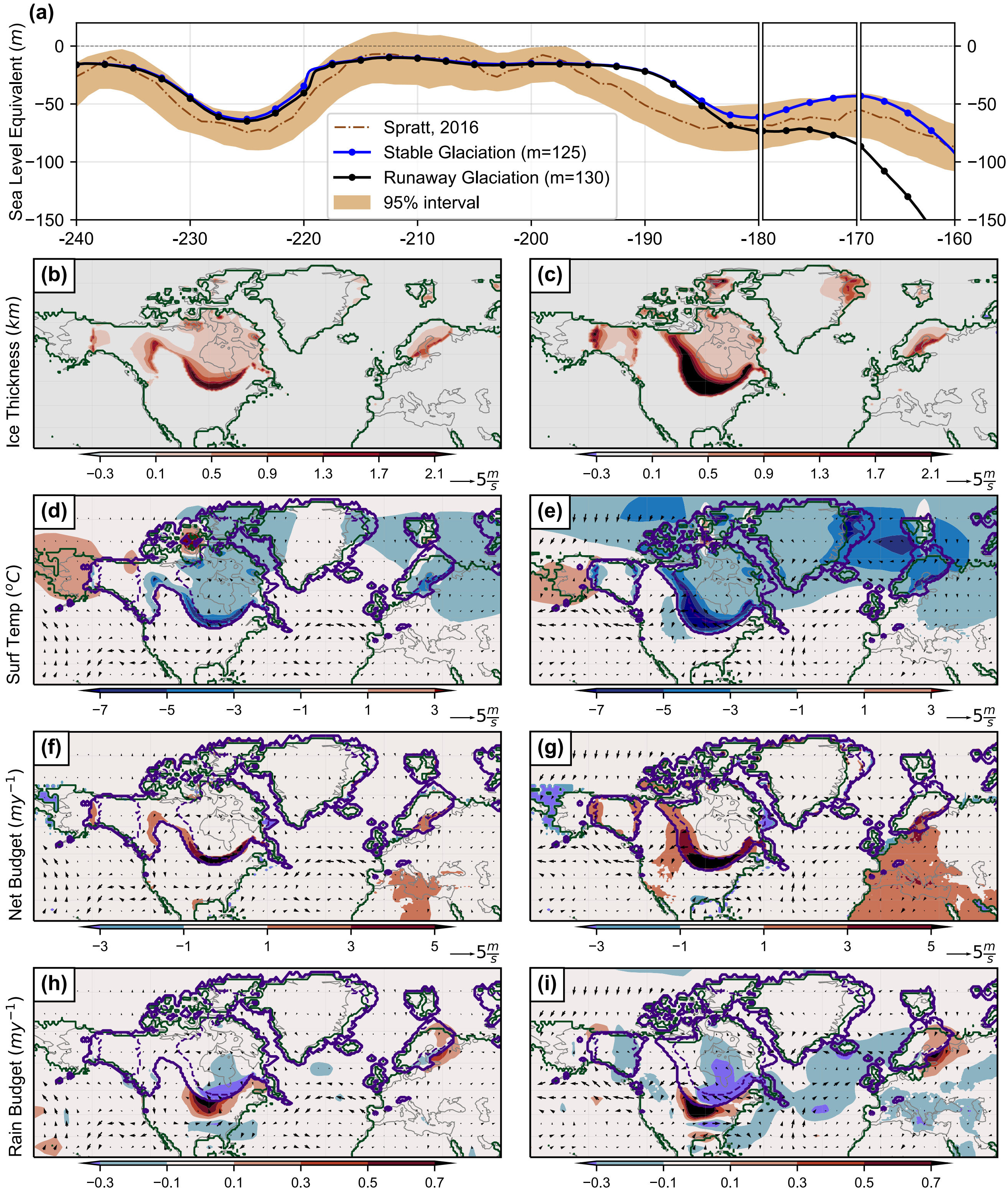

Figure S10: Difference between the simulations at the 180ka and 170ka over Laurentide. (a) Sea level reconstruction (m) and 95% confidence interval of Spratt and Lisiecki (2016) (brown). Total ice volume (in terms of SLE, m) from two ensemble members of LOVECLIP, one that leads to a stable glacial inception (blue; α=2, m=125 Wm^{-2}) and another into a runaway glaciation (black; α=2, m=130 Wm^{-2}). Difference in values between the runaway ensemble and the stable ensemble at 180ka (left column) and 170ka (right column) for (b,c) for ice thickness (solid colors, km); (d,e) surface temperature (°C) and winds at 800hPa (vectors, ms^{-1}); (f,g) net mass balance (my^{-1}) winds at 800hPa (vectors, ms^{-1}); and (h,i) rainfall (my^{-1}) winds at 800hPa (vectors, ms^{-1}). The solid and dashed purple lines in (d) to (i) mark the boundaries of the ice sheets from the runaway ensemble and the stable ensemble respectively. Solid green lines show the grounding line from the stable run. Anomalies over the Eurasian and Siberian ice sheets are small and not shown.

References:

Spratt, R. M., and Lisiecki, L. E.: A Late Pleistocene sea level stack, Climate of the Past, 12, 1079-1092, 2016.